

ASC Modulates CTL Cytotoxicity and Transplant Outcome Independent of the Inflammasome

Melody Cheong^{1,2}, Kate H. Gartlan^{1,3}, Jason S. Lee^{1,3}, Siok-Keen Tey^{1,4}, Ping Zhang¹, Rachel D. Kuns¹, Christopher E. Andoniu^{5,6}, Jose Paulo Martins¹, Karshing Chang¹, Vivien R. Sutton^{7,8}, Greg Kelly¹, Antiopi Varelias¹, Slavica Vuckovic^{3,9}, Kate A. Markey¹, Glen M. Boyle¹, Mark J. Smyth¹, Christian R. Engwerda¹, Kelli P.A. MacDonald¹, Joseph A. Trapani^{7,8}, Mariapia A. Degli-Esposti^{5,6}, Motoko Koyama^{1,10}, and Geoffrey R. Hill^{1,10}



ABSTRACT

The adaptor protein ASC (apoptosis-associated speck-like protein containing a CARD) is known to facilitate caspase-1 activation, which is essential for innate host immunity via the formation of the inflammasome complex, a multiprotein structure responsible for processing IL1 β and IL18 into their active moieties. Here, we demonstrated that ASC-deficient CD8⁺ T cells failed to induce severe graft-versus-host disease (GVHD) and had impaired capacity for graft rejection and graft-versus-

leukemia (GVL) activity. These effects were inflammasome independent because GVHD lethality was not altered in recipients of caspase-1/11-deficient T cells. We also demonstrated that ASC deficiency resulted in a decrease in cytolytic function, with a reduction in granzyme B secretion and CD107a expression by CD8⁺ T cells. Altogether, our findings highlight that ASC represents an attractive therapeutic target for improving outcomes of clinical transplantation.

Introduction

Allogeneic hematopoietic stem cell transplantation is the curative therapy for many malignant and nonmalignant hematologic diseases. However, graft-versus-host disease (GVHD) is a major complication following allogeneic bone marrow transplantation (BMT), resulting in mortality of approximately 20% of recipients (1). Acute GVHD develops early after transplant and is mediated by naïve donor T cells present within the graft (2). Subsequent pathophysiology is characterized by a cascade of immunologic interactions between antigen-presenting cells of both donor and recipient origin, CD4⁺ and CD8⁺ T cells, and further perpetuated by the continuous production of inflammatory effector molecules and a proinflammatory cytokine storm. A better understanding of these pathways is essential to minimize GVHD pathology. The increasing use of MHC-disparate grafts in clinical BMT

has meant that graft rejection is also an increasingly important issue. Graft rejection is predominantly mediated by recipient natural killer (NK) cells early after BMT (within 72 hours) and CD8⁺ T cells thereafter (3). Hence, effective approaches to overcome graft failure are also paramount for successful transplant outcome.

The discovery of Nod-like receptor (NLR) proteins triggered interest in their contribution to inflammation and, in particular, numerous autoimmune diseases (4). Inflammasomes are multiprotein complexes well-known for initiating innate immunity. Their formation requires three components: an NLR or HIN-200 receptor protein, a bipartite adaptor protein called apoptosis-associated speck-like protein containing a caspase recruitment domain (ASC; also known as Pycard), and pro-caspase-1 as the third and most distal component. ASC is primarily viewed as the link between the sensor protein and pro-caspase-1, although not always required (5), mediating full inflammasome assembly, and its activation dependent on MyD88 signaling (6). However, ASC has been shown to possess roles independent of the inflammasome, including regulating immune cell migration and antigen uptake (7), as well as other noninflammasome effects in host innate immunity (8, 9). Despite these studies, the role of ASC in GVHD and graft rejection has not been examined closely, although it is clear that the NLR protein 3 (NLRP3) inflammasome within recipient cells plays a role in initiating inflammation after conditioning and subsequent acute GVHD (10). The aim of this study was to identify the role of ASC expression in transplant outcome following BMT. We report that ASC promoted GVHD and graft rejection via enhancing cytotoxic function of donor or recipient CD8⁺ T cells, respectively.

¹QIMR Berghofer Medical Research Institute, Brisbane, Queensland, Australia.

²School of Natural Sciences, Griffith University, Nathan, Queensland, Australia.

³Faculty of Medicine, University of Queensland, Brisbane, Queensland, Australia.

⁴The Royal Brisbane and Women's Hospital, Brisbane, Queensland, Australia.

⁵Centre for Experimental Immunology, Lions Eye Institute, Nedlands, Western Australia, Australia.

⁶Infection and Immunity Program and Department of Microbiology, Biomedicine Discovery Institute, Monash University, Clayton, Victoria, Australia.

⁷Cancer Cell Death Laboratory, Peter MacCallum Cancer Centre, Melbourne, Victoria, Australia.

⁸Sir Peter MacCallum Department of Oncology, The University of Melbourne, Victoria, Australia.

⁹Institute of Haematology, Royal Prince Alfred Hospital, Sydney, New South Wales, Australia.

¹⁰Division of Clinical Research, Fred Hutchinson Cancer Research Center, Seattle, Washington.

Note: Supplementary data for this article are available at Cancer Immunology Research Online (<http://cancerimmunolres.aacrjournals.org/>).

Corresponding Author: Geoffrey R. Hill, Fred Hutchinson Cancer Research Center, Seattle, WA 98109. Phone: 120-6667-3324; Fax: 120-6667-5255; E-mail: grhill@fredhutch.org

Cancer Immunol Res 2020;8:1085-98

doi: 10.1158/2326-6066.CIR-19-0653

©2020 American Association for Cancer Research.

Materials and Methods

Mice

Female C57BL/6J (B6.WT, H-2^b, CD45.2⁺), B6.Ptprc^a (B6.Ptp, H-2^b, CD45.1⁺), B6.PtprcC57BL/6J [B6.CD45.1⁺CD45.2⁺ (H-2^b)], B6D2F1 (H-2^{b/d}), BALB/b (H-2^b), and BALB/c (H-2^d) mice were purchased from the Animal Resources Centre. The following mice were bred in-house at QIMR Berghofer (QIMRB) Medical Research Institute (Brisbane, Queensland, Australia): C57BL/6 ASC-deficient

Cheong et al.

(B6.ASC^{-/-}; ref. 11), B6.IL-1R^{-/-} (12), B6.NLRP3^{-/-} (13), B6.perforin^{-/-} (14), B6.MyD88^{-/-}/TRIF^{-/-} (Shizuo Akira; Osaka University, Suita, Osaka, Japan), and BALB/c.Luciferase⁺ (Remi Creusot; Stanford University, Stanford, CA). B6.caspase-1/11^{-/-}-deficient mice (15) were obtained from Drs. Kate Schroder and Katryn Stacey (University of Queensland, Queensland, Australia). All transgenic strains were backcrossed more than 10 times. Mice were between 6–12 weeks of age and housed in micro-isolator cages, and in cohousing experiments, were cohoused for 4 weeks prior to use. For engraftment studies, baytril (100 mg/L, Provet) was added to drinking water. All animal procedures were carried out with approval from the QIMRB Animal Ethics Committee.

BMT

Total body irradiation was administered on day 0 (¹³⁷Cs source at 108 cGy/minute), split into two doses separated by 3 hours, to B6D2F1 (1,100–1,300 cGy) and BALB/b and BALB/c mice (900 cGy). On day 0, lethally irradiated mice were transplanted with 5 × 10⁶ B6 whole or T-cell-depleted (TCD) bone marrow (BM) with or without 2 × 10⁶ (B6D2F1 recipients), 5 × 10⁶ (BALB/b recipients), or 0.5 × 10⁶ (BALB/c recipients) purified splenic T cells. TCD grafts containing only 5 × 10⁶ TCD BM were transplanted in non-GVHD controls. In engraftment experiments, B6 recipients were lethally irradiated on day -1 (1,000 cGy) and transplanted with 10⁶ luciferase-positive BALB/c BM on day 0. GVHD was assessed using a cumulative scoring system (16). The scores of systemic GVHD were based on the following five clinical parameters: weight loss, posture (hunching), activity, fur texture, and skin integrity (maximum index = 10). Mice were sacrificed in accordance with institutional animal ethics guidelines and the date of death deemed as the next day.

Bioluminescence imaging

Donor hematopoietic stem cell expansion was measured weekly via luciferase signal intensity using the Xenogen IVIS 100 (Caliper Life Sciences). Mice were anesthetized with isoflurane (Provet) and injected with 500 µg of D-luciferin (PerkinElmer) subcutaneously, and then imaged 5 minutes later.

In vivo cytotoxicity assays

On day 12 posttransplant, mice received 20 × 10⁶ congenic donor-type B6 (CD45.1⁺)–unlabeled splenocytes and 20 × 10⁶ host-type B6D2F1 carboxyfluorescein diacetate succinimidyl ester (CFSE)–labeled splenocytes. For CFSE labeling, splenocytes were resuspended in serum-free media, before adding CFSE (Sigma-Aldrich) at a final concentration of 1 µmol/L. Cells were incubated at 37°C for 10 minutes and then washed with 2% FCS containing RPMI. In engraftment experiments, irradiated recipients were coinjected with 12 × 10⁶ B6.CD45.1⁺CD45.2⁺ BM cells and 12 × 10⁶ BALB/c CD45.1⁺ BM cells. Animals were sacrificed 18 hours later and spleens harvested, mashed in 2% FCS containing RPMI, and then filtered for single-cell suspensions. Splenocytes were stained with anti-CD45.1-PE. The index of cytotoxicity against recipient cells was calculated as the percentage of CD45.1⁺ (donor-type) cells to remaining CFSE⁺ (host-type) cells.

In vivo depletion in BMT

Regulatory T cell (Treg) depletion was performed by injecting 500 µg anti-CD25 (PC61, in-house) or Mac49 IgG1 control antibody (in-house) intraperitoneally on days -3 and -1. For donor CD8⁺ T-cell depletion experiments, B6.WT or B6.ASC^{-/-} donors were treated with or without 150 µg CD8β antibody (53-5.8, in-house) intrave-

nously on days -3 and -1, and recipients were treated on day +3. For recipient CD8⁺ T-cell depletion, recipients were treated with or without 150 µg CD8β antibody intravenously pre- and posttransplant (days -3, -1, +1, and +7). For NK-cell depletion experiments, recipients were treated with 1 mg NK1.1 antibody (PK136, in-house) intraperitoneally on days -2 and 0.

Primary leukemia and cell line

The primary myeloid blast crisis chronic myeloid leukemia (GFP⁺, H2^{b/d}, and CD45.2⁺) created by the fusion of *BCR/ABL-NUP98/HOXA9* genes was generated as described previously (17). Tumor was propagated in irradiated (day -1) B6D2F1 mice using a murine syngeneic model (B6D2F1 → B6D2F1). On the day of the transplant, recipients received 5 × 10⁶ TCD BM and 10⁶ tumor cells. Spleens were harvested on day 10 post-BMT and splenocytes prepared into single-cell suspensions by washing twice and resuspending in culture media before cryopreservation for *in vivo* use. For mouse cytomegalovirus (MCMV) studies, the M210B4 mouse fibroblast cell line used for plaque assays was grown as described previously (18).

Cell preparations

T cells were purified using magnetic bead depletion of non-T-cell splenocytes bound to rat-originated mAbs (anti-CD19: HB305; anti-B220:RA36B2; anti-GR1: RB6-8C5; anti-Ter119: Ter119; and anti-CD11b: TIB128), after which cells were incubated with goat anti-rat IgG BioMag Beads (Qiagen) as described previously (19). CD3⁺ T-cell purities were >80%. For total T-cell depletion, splenocytes were incubated with hybridoma supernatants containing anti-CD4 (RL172), anti-CD8 (TIB211), and Thy1.2 (HO-13-4) mAb, followed by incubation with rabbit complement (Cedarlane Laboratories) as described previously (20). In some experiments, splenic CD4⁺ cells (>80% CD4⁺CD3⁺ and ≤1% CD8⁺CD3⁺) or CD8⁺ cells (>80% CD8⁺CD3⁺ and <1% CD4⁺CD3⁺) were purified using CD4 (L3T4) and CD8 (Ly-2) MicroBeads, respectively, together with positive Selection Columns (Miltenyi Biotec). CD25⁺CD4⁺ cells (>97% purity) were purified from spleen by cell sorting on the basis of CD8⁻, CD25⁺, and 7-aminoactinomycin D (7AAD) expression (FACS Aria, Becton Dickinson) following CD4⁺ cell selection using the MACS system as described earlier. For sorting experiments, cells were sorted to ≥97% purity. To investigate the effect of Tregs, 0.2 × 10⁶ sorted splenic CD25⁺CD8⁻ Tregs from naïve B6.WT or B6.ASC^{-/-} donors were transplanted with B6.WT TCD BM into lethally irradiated BALB/c recipients on day 0. Two days later, 0.5 × 10⁶ CD3⁺ T cells from anti-CD25–treated B6.WT donors were transferred.

Hybridoma generation

Hybridomas were expanded up to T175 flasks, where they were grown to confluency in 2% FCS containing RPMI. Each flask was transferred to a 1 L roller bottle, and over several days, the volume increased to 1 L with serum-free RPMI. Roller bottles were grown for a further 21 days. Supernatants were filtered to remove cellular debris. Protein was collected from supernatants by ammonium sulphate precipitation, and IgG antibodies purified using a protein G column. Purified antibodies were dialyzed, concentrated, and filter sterilized to a concentration of 5 mg/mL in PBS.

Antibodies and flow cytometric analysis

The following antibodies were purchased from BioLegend: FITC-conjugated anti-H-2D^b (KH95), phycoerythrin (PE)-conjugated CD3 (145-2C11), CD19 (6D5), CD44 (1M7), CD45.1 (A20), Alexa Fluor (AF) 700-conjugated CD62L (MEL14), allophycocyanin (APC)-

ASC Modulates Inflammation-Independent CTL Cytotoxicity

conjugated CD45.2 (104), Brilliant Violet (BV) 605 CD90.2 (53-2.1), and CD3 (17A2). The following antibodies were purchased from BD Biosciences: PE-conjugated CD25 (7D4), peridinin chlorophyll protein (PerCP) Cy5.5-conjugated CD8 (53-6.7), Pacific Blue-conjugated CD4 (RM4-5), allophycocyanin cyanine7 (APC-Cy7)-conjugated Ly6G (1A8), violet 450-conjugated CD107a (1D4B), and rat IgG2a isotype control and biotin-conjugated H-2D^d. FITC-conjugated CD8 (53-6.7) was generated in-house. Foxp3 was detected with Alexa Fluor 647-conjugated Foxp3 (150D) and the Foxp3 Staining Buffer Set (eBioscience) according to the manufacturer's protocol. Prior to staining, 50 μ L of 2.4G2 antibody (generated in-house) was added to cells for 10 minutes at room temperature to block Fc γ receptors. Cells were then incubated with antibodies accordingly for 20 minutes on ice, then washed, and resuspended in PBS containing 2% FCS and 5 mmol/L EDTA. All samples (days 12, 21, and 30 posttransplant) were acquired on a BD LSR Fortessa (BD Biosciences) using BD FACSDiva (v7.0) and analyzed with FlowJo (v9.7).

Leukemia challenge

All assays were undertaken as described previously (21). Briefly, recipients were injected intravenously with 10⁶ GFP-transfected BCR/ABL-NUP98/HOXA9 tumor cells on the same day of transplantation. The tumor cells obtained were generated as described previously (17). Survival and GVHD clinical scores were monitored. Peripheral blood was collected weekly in the first 4 weeks and fortnightly thereafter by retro-orbital bleed into Vacuette K2E K2EDTA Tubes (Greiner Bio-One) to prevent coagulation. Blood samples were then counted on a Coulter counter, and red blood cells lysed with Gey's red cell lysis buffer (produced in-house). Leukemia burden was measured on days 7, 14, 18, and 21, and subsequently weekly by determining the number of GFP⁺ cells via flow cytometry (LSR Fortessa). Leukemia burden was also determined at the time of termination (day 63) by collecting peripheral blood, BM, and spleens and analyzed by flow cytometry.

Microarray for gene expression profiling

Transcriptional profiling was performed on sorted, as indicated above, CD8⁺ T cells from recipient mice transplanted with B6.WT or B6.ASC^{-/-} BM and T cell grafts. Dead cells were excluded via 7AAD. RNA for microarray analysis was extracted using the RNeasy Micro Kit (Qiagen) and any contaminating genomic DNA was removed with DNase I (Qiagen) treatment per the manufacturer's protocol. Preparations were checked for RNA integrity by Agilent 2100 Bioanalyzer (RIN 6.3–9.1). mRNA was amplified and biotinylated with the Illumina TotalPrep RNA Amplification Kit (Life Technologies) before hybridization to Mouse Ref-8 v2.0 Expression Bead Chip arrays as per the manufacturer's instructions. Chips were read via iScan Microarray Scanner (Illumina) and analyzed using GenomeStudio (Illumina) and GeneSpring GX v12.5 (Agilent Technologies) software. Pathway analyses were performed using Ingenuity Pathway Analysis (IPA; Ingenuity, Qiagen). The microarray dataset has been deposited to the NCBI Gene Expression Omnibus under accession number GSE78755.

Western blotting

Cell pellets of 1–5 \times 10⁶ sort-purified splenic CD8⁺CD90.2⁺ T cells from day 12 posttransplant recipients, which received B6.WT or B6.ASC^{-/-} or B6.perforin^{-/-} grafts, were resuspended in lysis buffer (50 mmol/L Tris pH 7.6, 250 mmol/L NaCl, 5 mmol/L EDTA pH 8, 50 mmol/L NaF, and 50 mmol/L PMSF). Supernatant of the cell lysate was collected, and protein quantification was measured using the Bio-Rad Protein Assay Dye (Bio-Rad). Protein samples were resolved on

4%–15% precast polyacrylamide gels (Bio-Rad), and protein bands transferred by wet transfer onto a polyvinylidene difluoride membrane. The membrane was blocked with 5% (w/v) skim milk (sourced locally) for 1 hour and incubated with anti-mouse perforin (Abcam) at 1:1,000 dilution overnight at 4°C. Subsequently, the membrane was washed with 0.1% (v/v) PBS-Tween and incubated with a polyclonal goat anti-rat horseradish peroxidase (Abcam) secondary antibody at 1:3,000 dilution for 1 hour and then washed. Membranes were developed by ECL Substrate (Bio-Rad) and detected by chemiluminescence on a DNR Chemi Bis Imager (DKSH).

Cytokine analysis

Day 7 retro-orbital bleeds of B6D2F1 recipients transplanted with BM and T cells from B6.WT, B6.ASC^{-/-}, or B6.caspase-1/11^{-/-} donor mice or B6.WT TCD BM only were collected in Eppendorf tubes. Blood samples were allowed to clot before being spun at 10,000 rpm for 10 minutes and then sera were collected. Serum cytokines were determined using the BD Cytometric Bead Array System and analyzed on the BD FACSAArray Bioanalyzer System (BD Biosciences) according to the manufacturer's protocol. *Ex vivo*, splenocytes were stimulated with phorbol 12-myristate 13-acetate (PMA; 50 ng/mL, Sigma-Aldrich) and ionomycin (500 ng/mL, Sigma-Aldrich), and Brefeldin A (1:1,000 dilution; BioLegend) for 4 hours in culture medium: Iscove's Modified Dulbecco's Media (Life Technologies) supplemented with 10% FCS, 1% penicillin/streptomycin (Life Technologies), 1% L-glutamine (Thermo Fisher Scientific), 1% nonessential amino acids (Life Technologies), 1% sodium pyruvate (Sigma-Aldrich), 1% HEPES (Life Technologies), and 0.02 mmol/L β -mercaptoethanol (Sigma-Aldrich). For CD107a staining (day 12, 21, and 30), splenocytes were additionally cultured with monensin (1/1,000 dilution; BioLegend) and anti-CD107a or isotype control for 5 hours at 37°C. Stained cells were processed for intracellular cytokine staining per the manufacturer's protocol (BD Cytofix/Cytoperm Kit; BD Bioscience) and analyzed by flow cytometry, as indicated above.

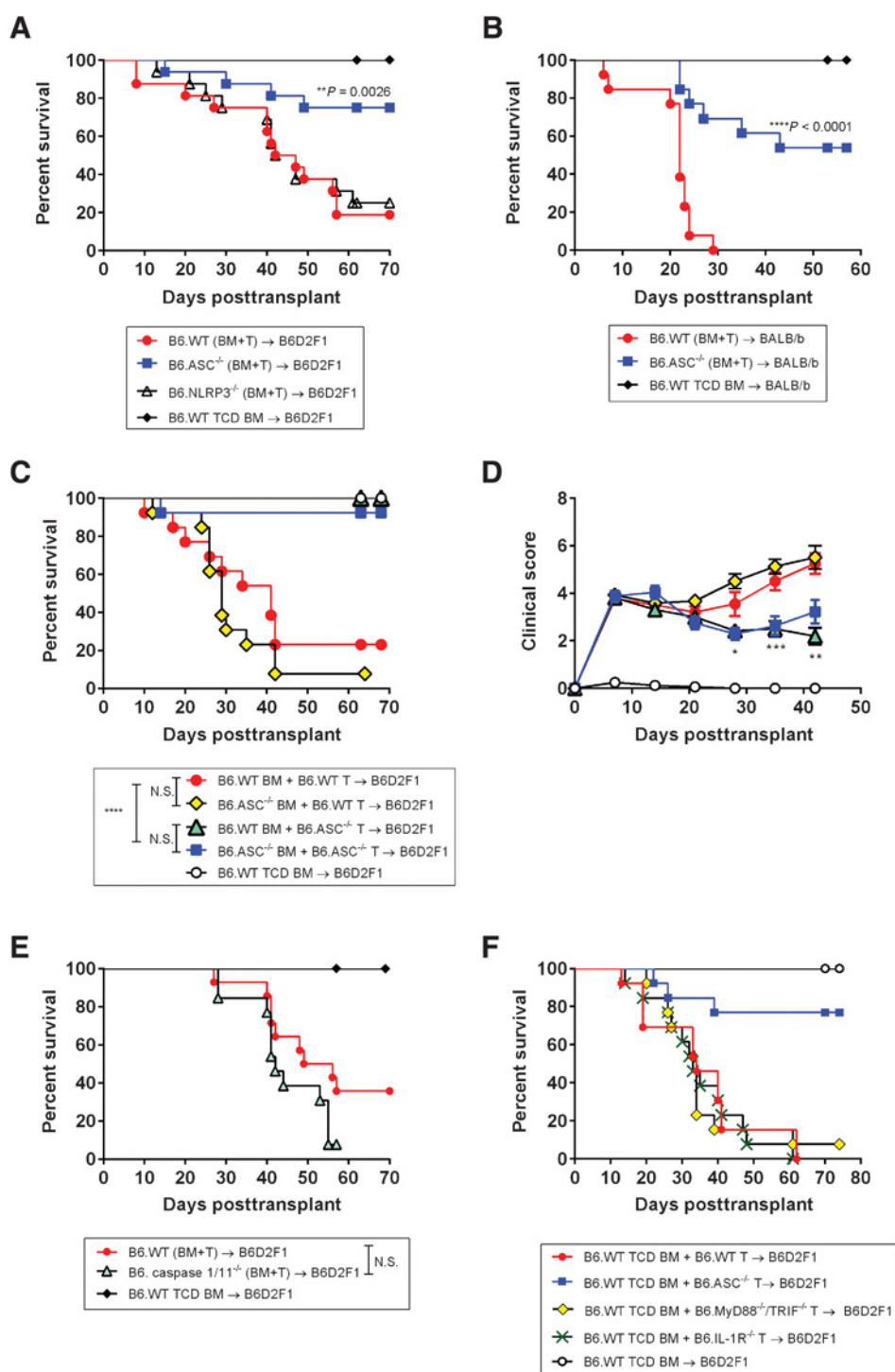
Granzyme B ELISA

Secretion of granzyme B in tissue culture supernatant was quantified using the mouse Granzyme B ELISA Ready-SET-Go Kit (eBioscience). Sorted splenic CD8⁺ T cells from mice transplanted 12 days earlier (as described for microarray analysis) were seeded at 1.5 \times 10⁶/mL in culture medium (as described above) and stimulated with PMA (50 ng/mL) and ionomycin (500 ng/mL) for 6 hours. Culture medium was then harvested, centrifuged to remove cellular debris, and 100 μ L assayed in accordance with the manufacturer's instructions. Absorbance readings (405 nm) were determined using a Benchmark Microplate Reader (Bio-Rad) using the Softmax Pro Software (Molecular Devices). The concentration of granzyme B was quantified on the basis of the standard curve generated using the standards (40–5,000 pg/mL) provided by the manufacturer.

MCMV studies

B6D2F1 mice were inoculated intraperitoneally with 1 \times 10⁴ plaque-forming units (PFU) of salivary gland propagated (SGV) MCMV-K181Perth virus (22). Mice were housed for approximately 3 months until the establishment of MCMV latency, as described previously (23). Latently infected mice were lethally irradiated and transplanted with 5 \times 10⁶ BM and 2 \times 10⁶ CD3⁺-purified T cells from noninfected B6.WT and B6.ASC^{-/-} mice. Reactivation was measured by plasma viremia using a qRT-PCR assay for the viral glycoprotein B (*gB*) gene (23). Briefly, whole blood was collected from the retro-orbital sinus at day 27 post-BMT and transferred into a microfuge tube

Cheong et al.

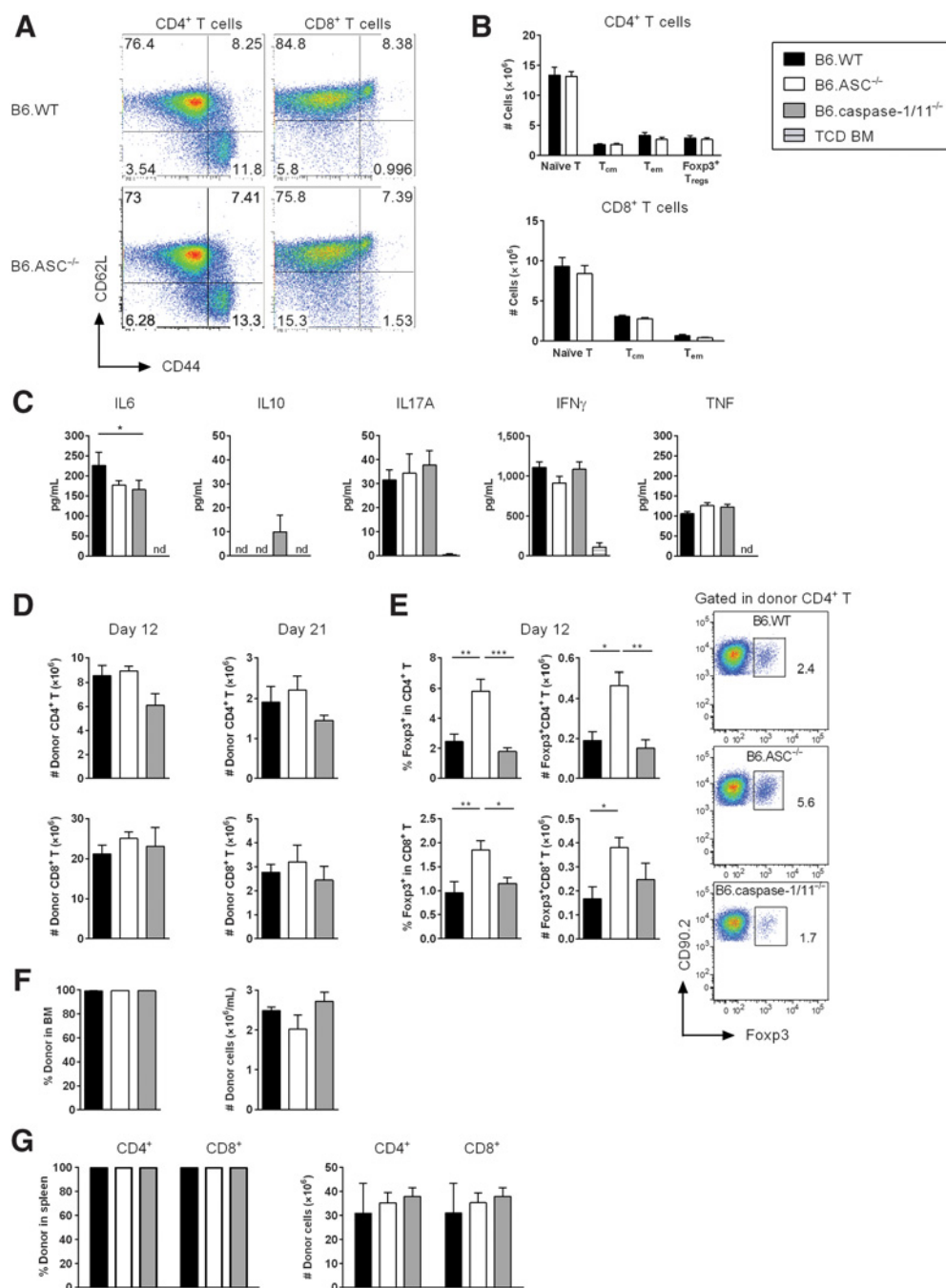
**Figure 1.**

ASC in donor T cells mediates GVHD independently of the inflammasome. **A**, Lethally irradiated B6D2F1 recipients were transplanted with BM and T cells from B6.WT, B6.NLRP3^{-/-}, or B6.ASC^{-/-} donors and monitored for GVHD thereafter. The control non-GVHD group received TCD BM only. **, $P = 0.0026$, B6.ASC^{-/-} versus B6.WT. Results combined from two replicate experiments ($n = 16$ per T-cell-replete group, $n = 8$ for TCD group). **B**, Survival of lethally irradiated BALB/b recipients transplanted as detailed in Materials and Methods. ****, $P < 0.0001$, B6.ASC^{-/-} versus B6.WT. Results combined from two replicate experiments ($n = 13$ per T-cell-replete group, $n = 8$ for TCD group). **C** and **D**, B6.WT or B6.ASC^{-/-} TCD BM was mixed with FACS-purified B6.WT or B6.ASC^{-/-} CD90.2⁺ T cells and transplanted into B6D2F1 recipients. Non-GVHD control cohort received TCD BM only. Results combined from two replicate experiments ($n = 13$ per T-cell-replete group, $n = 9$ for TCD group). GVHD survival (**C**) and clinical scores (**D**) are shown. *, $P = 0.01$; **, $P = 0.004$; ***, $P = 0.0003$, B6.WT BM + B6.ASC^{-/-} T versus B6.WT BM + B6.WT T cells. ****, $P < 0.0001$, B6.WT BM + B6.ASC^{-/-} T versus B6.WT BM + B6.WT T cells and B6.ASC^{-/-} BM + B6.WT T versus B6.ASC^{-/-} BM + B6.ASC^{-/-} T cells. N.S., not significant. **E**, Survival of B6D2F1 recipients that received B6.WT or B6.caspase-1/11^{-/-} BM + T-cell donor grafts. Data shown are combined from two replicate experiments ($n = 14$ per T-cell-replete group, $n = 8$ for TCD group). N.S., not significant. **F**, Survival curves of B6D2F1 recipients transplanted with B6.WT TCD BM and FACS-sorted T cells from B6.WT, B6.ASC^{-/-}, B6.MyD88^{-/-}/TRIF^{-/-}, or B6.IIL1R^{-/-} donor mice. Data shown are from two replicate experiments ($n = 13$ per T-cell-replete group, $n = 6$ for TCD group). Survival curves were plotted using Kaplan-Meier estimates and compared by log-rank analysis. Clinical scores for B6.WT BM + B6.ASC^{-/-} T versus B6.WT BM + B6.WT T cells were analyzed by Mann-Whitney U test (unpaired, two-tailed). Results are presented as mean \pm SEM.

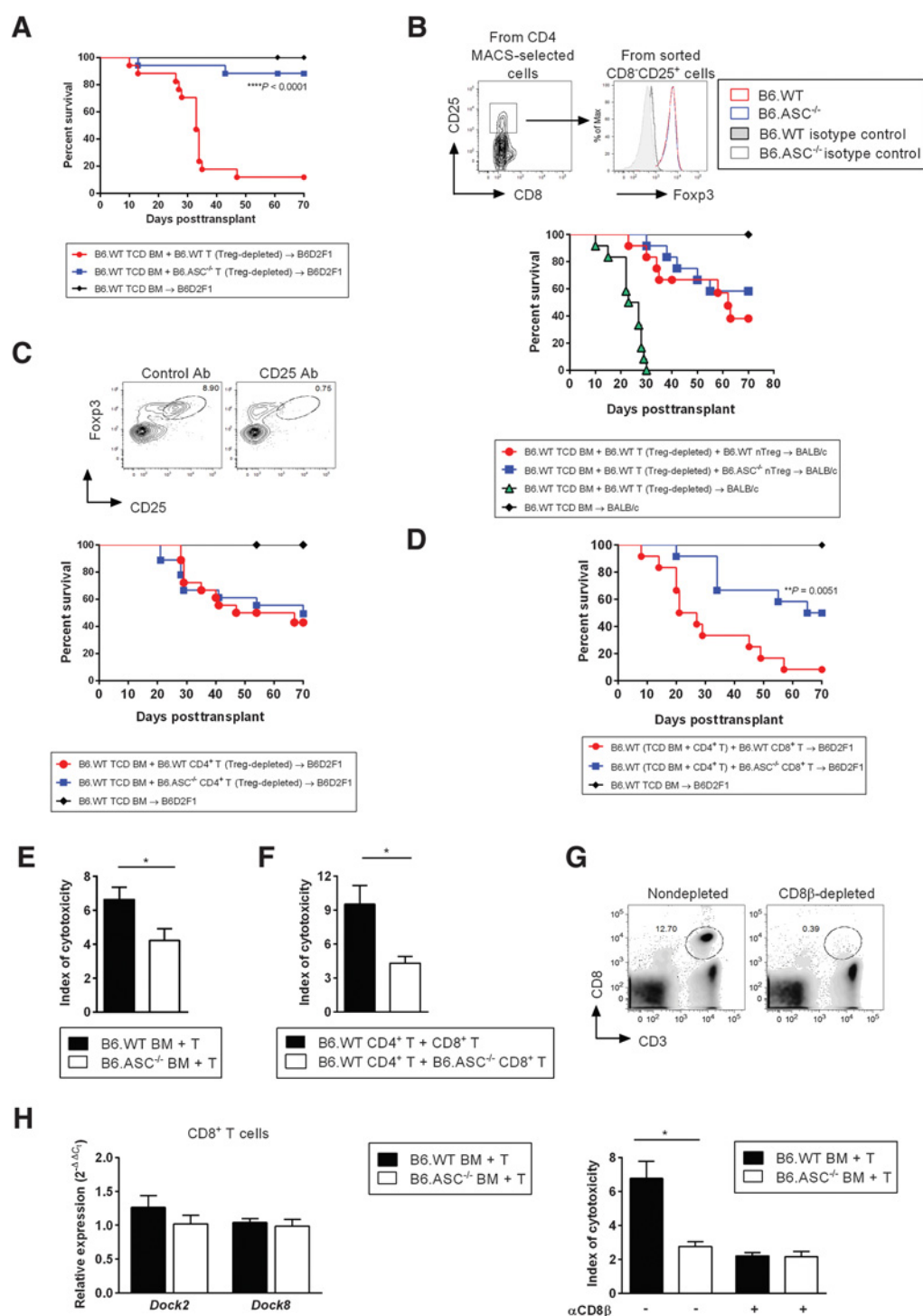
containing 10 μ L of 500 mmol/L EDTA. Tubes were centrifuged at 14,000 rpm for 5 minutes and plasma collected. Qiagen DNeasy Blood and Tissue Kit (Qiagen) was used to harvest DNA from plasma as per the manufacturer's protocol. Quantitative PCR to detect the *gB* gene of MCMV was performed using specific primers (F: 5' TTGGCTGTCGTCTAGCTGTTT 3' and R: 5' TAAGCGGTGGAC-TAGCGATAA 3') and the Sso Advanced Universal SYBR Green System (Bio-Rad). Serial dilutions of a synthesized MCMV *gB*

sequence were used to generate a standard curve. Spleen, liver, and lung tissues were also collected and viral loads measured by plaque assay using M210B4 cell monolayers (24). Tissues were homogenized, serial dilutions prepared, and 200 μ L of each dilution added onto 24-well tissue culture trays containing subconfluent M210B4 cell monolayers. After incubating at 37°C for 1 hour, the homogenates were removed by aspiration and cells overlaid with 0.01% carboxymethylcellulose (Sigma-Aldrich). The trays were then incubated at

ASC Modulates Inflammasome-Independent CTL Cytotoxicity

**Figure 2.**

Donor Foxp3⁺ Tregs are increased in recipients of ASC^{-/-} grafts. **A**, Representative flow cytometry plots of splenic CD4⁺ and CD8⁺ naïve (CD62L^{hi}CD44^{neg}), effector memory (CD62L^{lo}CD44^{hi}), and central memory (CD62L^{hi}CD44^{hi}) T cells in naïve B6.WT and B6.ASC^{-/-} donors. **B**, Numbers of T-cell subsets, as defined in **A**, Tregs, and naïve T cells ($n = 8$ per group). Results combined from two replicate experiments. Tcm, central memory T cell; Tem, effector memory T cell. **C**, Serum cytokines (IL6, IL10, IL17A, IFN γ , and TNF) at day 7 posttransplant in B6D2F1 recipients transplanted with BM and T cells from B6.WT, B6.ASC^{-/-}, or B6.caspase-1/11^{-/-} donor mice or B6.WT TCD BM only (day 7: $n = 6$ per T-cell-replete group, $n = 3$ per TCD BM group). Results are from one experiment. nd, not detectable. **D**, Absolute number of donor splenic CD4⁺ and CD8⁺ T cells 12 and 21 days after transplant. **E**, Frequency and absolute number of Foxp3⁺ cells in spleens at day 12 post-BMT shown with representative plots. Data combined from two replicate experiments ($n = 10$ per T-cell-replete group and $n = 3$ in TCD for each time point). **F** and **G**, Percentage and absolute numbers of donor cells in BM and spleen ($n = 3-4$ per group) on day 12 posttransplant. Data are from one experiment. Results in **B** were analyzed by Mann-Whitney U test (unpaired, two-tailed). Data in **C-E** were analyzed using one-way ANOVA (Tukey multiple comparison test) for multiple test comparisons when data were normally distributed. For data that were not normally distributed, Kruskal-Wallis test (Dunn multiple comparison test) was used for multiple group comparisons. *, $P < 0.05$; **, $P < 0.01$; ***, $P < 0.001$. Results are presented as mean \pm SEM.

**Figure 3.**

Donor CTL function is significantly reduced in ASC-deficient-grafted mice. **A**, Lethally irradiated B6D2F1 were transplanted with B6.WT TCD BM and whole T cells from CD25-treated B6.WT or B6.ASC^{-/-} donors on day 0. Non-GVHD mice were transplanted with B6.WT TCD BM. Data combined from three replicate experiments ($n = 17$ per T-cell-replete group, $n = 9$ for TCD group). ****, $P < 0.0001$, B6.ASC^{-/-} versus B6.WT. **B**, Purified Tregs from B6.WT or B6.ASC^{-/-} mice were transplanted along with B6.WT TCD BM into BALB/c recipients on day 0. Two days later, T cells from Treg-depleted B6.WT donors were transferred. The GVHD control group received TCD BM + T cells without Tregs, whereas the non-GVHD group received only TCD BM. Survival of transplanted mice and representative plots of purified CD8⁺CD25⁺ cells (Tregs) are shown. Data are combined from two replicate experiments ($n = 12$ per T-cell-replete group, $n = 6$ for TCD). **C**, Survival of mice as in **A** but using purified CD4⁺ T cells from CD25- or control mAb-treated B6.WT or B6.ASC^{-/-} donors (representative plots are shown). Data are combined from three replicate experiments ($n = 18$ per T-cell-replete group, $n = 9$ for TCD). **D**, Survival of B6D2F1 recipients transplanted with B6.WT TCD BM and B6.WT CD4⁺ T cells plus B6.WT or B6.ASC^{-/-} CD8⁺ T cells. Data are combined from two independent experiments ($n = 12$ per T-cell-replete group, $n = 8$ per TCD group). (Continued on the following page.)

ASC Modulates Inflammasome-Independent CTL Cytotoxicity

37°C for 4 days, fixed, and stained with 0.5% methylene blue in 10% formaldehyde for 1 day prior to plaques being counted. PFU per organ calculated was calculated as number of plaques counted \times 5 (as 200 μ L was added per well) \times dilution factor \times number of mL organ was homogenized in.

qRT-PCR

RNA from B6D2F1 recipients transplanted 12 days earlier with B6.WT or B6.ASC^{-/-} BM and T cells was extracted using the RNeasy Micro Kit (Qiagen) per the manufacturer's protocol and any contaminating genomic DNA was removed with DNase I (Qiagen) treatment, as already described above. cDNA was prepared with Maxima H Minus First Strand cDNA Synthesis Kits (Thermo Fisher Scientific). Assays were performed using 5 to 20 ng of cDNA template and TaqMan Primers (Thermo Fisher Scientific): Dock2 (Mm00473720_m1) and Dock8 (Mm00613802_m1) and run in duplicate on an ABI Viia7 Thermal Cycler (Applied Biosystems). Expression levels were determined using the comparative C_t method (2^{- $\Delta\Delta$ C_t}) normalized to the *Hprt* housekeeping gene.

Statistical analysis

Data were analyzed using GraphPad Prism (v6.07). Survival curves for GVHD were plotted using Kaplan–Meier estimates and compared by log-rank analysis. Leukemia death was analyzed using cumulative incidence analysis of competing risks by R_2.10.1 software. Differential gene expression by microarray was assessed by unpaired Student *t* test ($P < 0.05$) and subsequently FDR (Benjamini–Hochberg) correction and supervised hierarchical clustering performed after test. IPA and selection of immunologically relevant genes were generated from genes with >1.2-fold change in expression and $P < 0.05$ prior to FDR correction. One-way ANOVA (Tukey multiple comparison test) was used for multiple test comparisons when data were normally distributed. For data that were not normally distributed, Kruskal–Wallis test (Dunn multiple comparison test) was used for multiple group comparisons or Mann–Whitney U tests (two-tailed) for comparisons of two groups.

Results

ASC promotes transplant-related mortality independent of the inflammasome

To study the effect of the donor inflammasome on acute GVHD, lethally irradiated B6D2F1 recipients were transplanted with BM and T cells from MHC-mismatched B6.WT or B6.ASC^{-/-} mice. Seventy-five percent of the recipients receiving T-cell-replete B6.ASC^{-/-} grafts survived beyond day 70 posttransplant compared with less than 20% of the recipients transplanted with T-cell-replete wild-type (WT) grafts (Fig. 1A). In contrast, recipients of B6.NLRP3^{-/-} grafts had near identical GVHD to recipients of WT grafts (Fig. 1A). We also

confirmed the same phenomenon in a B6→BALB/b MHC-matched model, where GVHD is directed to multiple minor histocompatibility antigens (Fig. 1B). We also studied the effect of the recipient inflammasome on GVHD outcome and found that B6.NLRP3^{-/-} recipients, but not B6.ASC^{-/-} recipients, resulted in less mortality than B6.WT recipients (Supplementary Fig. S1). We next determined whether donor ASC expression in the BM or T-cell compartment was important for this exacerbation of GVHD by transplanting grafts in which BM, T cells, or combinations thereof were ASC^{-/-}. These studies demonstrated that GVHD was attenuated only when ASC was absent in the T-cell compartment, whereas ASC expression in the BM was irrelevant to GVHD severity (Fig. 1C and D). Because caspase-1 is the third and most distal component of the inflammasome complex, we utilized caspase-1-knockout mice to determine whether these results were inflammasome dependent. Transplantation of B6D2F1 recipients with B6.WT or B6.caspase-1/11^{-/-} BM, with or without T cells, demonstrated that the absence of caspase-1 did not reproduce the ASC^{-/-} survival advantage, suggesting that ASC is involved in an alternate inflammasome-independent pathway (Fig. 1E). Caspase-1/11^{-/-} mice lack both caspase-1 and -11, and their close proximity in the genome precludes their segregation by recombination (25), such that we excluded both canonical and noncanonical inflammasome pathways, respectively, by their use. We next transplanted recipients with either MyD88/TRIF- or IL1 receptor (IL1R)-deficient T cells to further confirm this result. Consistent with the absence of caspase-1/11, the absence of MyD88/TRIF within T cells, a set of adaptor molecules required for Toll-like receptor (TLR) signaling which abrogates whole TLR signaling, including subsequent pro-IL1 β and pro-IL18 production, did not reproduce the ASC^{-/-} phenotype. Similarly, IL1 signaling of donor T cells (lacking IL1R expression) was not required for the induction of GVHD lethality (Fig. 1F). Taken together, these data suggested that the donor cell ASC expression, which exacerbated GVHD, does not signal via the canonical inflammasome activation pathway in T cells.

ASC deficiency does not impact proinflammatory cytokine production

We next sought to examine how ASC deficiency controls GVHD. First, we excluded major defects in numbers of naïve (CD62L^{hi}CD44^{neg}), central memory (CD62L⁺CD44⁺) and effector/effector memory (CD62L^{neg}CD44⁺), and splenic CD4⁺ and CD8⁺ Foxp3⁺ Tregs in B6.ASC^{-/-} donor mice (Fig. 2A and B). We proceeded to analyze donor effector T cells and inflammatory cytokine production after allogeneic BMT. In the B6 → B6D2F1 model, systemic inflammatory cytokines at day 7 after transplant were equivalent in the recipients of B6.WT, B6.ASC^{-/-}, and B6.caspase-1/11^{-/-} grafts, whereas IL10 was not consistently detected above background in any of the groups (Fig. 2C). Subsequent analysis also revealed similar numbers of splenic donor CD4⁺ or CD8⁺ T cells at

(Continued.) **, $P = 0.0051$. **E**, B6D2F1 recipients were transplanted with BM and T cells from B6.WT or B6.ASC^{-/-} donors. On day 12, animals were coinjected with equal numbers of donor-type PTP (CD45.1⁺)- and CFSE-labeled host-type B6D2F1 splenocytes, and spleens were isolated 18 hours later. Index of cytotoxicity was determined by the ratio of donor-type (CD45.1⁺) to remaining host-type (CFSE⁺) cells in the spleen via flow cytometry. Results are combined from two identical experiments ($n = 8$ –9 per group). *, $P = 0.0152$. **F**, B6D2F1 recipients were transplanted with B6.WT TCD BM and MACS-purified CD4⁺ T cells from B6.WT donors together with B6.WT or B6.ASC^{-/-} MACS-selected CD8⁺ T cells. *In vivo* cytotoxicity assays were performed and analyzed as described in **E**. Data shown are combined from three replicate experiments ($n = 14$ –15 per group). *, $P = 0.0137$. **G**, B6D2F1 were transplanted with B6.WT or B6.ASC^{-/-} CD8⁺ TCD or T-cell-replete grafts. Representative plots of CD8⁺ T-cell depletion shown. On day 12 after BMT, *in vivo* cytotoxicity assays were performed and analyzed as described in **E**. Results are combined from two replicate experiments ($n = 8$ per control group, $n = 10$ per CD8-depleted group). *, $P = 0.034$. **H**, Naïve splenic B6.WT or B6.ASC^{-/-} CD8⁺ T cells were analyzed for *Dock2* and *Dock8* mRNA expression. Data combined from two replicate experiments ($n = 8$ per group). Survival curves in **A**–**D** were plotted using Kaplan–Meier estimates and compared by log-rank analysis. Data in **E**–**H** were analyzed by Mann–Whitney U test (unpaired, two-tailed). All data are presented as mean \pm SEM and $P < 0.05$ considered statistically significant.

days 12 and 21 after BMT (Fig. 2D). A significant expansion in both frequency and absolute numbers of donor Foxp3⁺ Tregs was seen in the spleens of recipients of B6.ASC^{-/-} grafts at day 12 after transplant (Fig. 2E). We also demonstrated that donor cells were fully engrafted in the BM (Fig. 2F), and the donor chimerism and reconstitution of CD4⁺ and CD8⁺ T cells were equivalent in the spleens between those recipients (Fig. 2G). Together, these data demonstrated that B6.caspase-1/11^{-/-} grafts did not phenocopy the protection from GVHD seen after transplantation of B6.ASC^{-/-} grafts, and the latter is associated with a significant expansion of donor Tregs.

Improved GVHD outcome in ASC-deficient mice is not due to donor Treg expansion

Having observed an increase in donor Tregs within ASC^{-/-}-transplanted recipients, we first tested whether this population was responsible for GVHD attenuation by performing T-cell-replete transplants with or without Tregs. We transplanted B6D2F1 recipients with B6.WT TCD BM and T cells from Treg-depleted B6.WT or B6.ASC^{-/-} donors (Fig. 3A). This demonstrated the protective effect of B6.ASC^{-/-} T cells despite the absence of Tregs (Fig. 3A). Next, we verified donor Treg function in the presence or absence of ASC by transplanting lethally irradiated BALB/c recipients with TCD BM from B6.WT mice with or without sorted CD25⁺CD4⁺ T cells (>90% Foxp3⁺; Fig. 3B) from B6.WT or B6.ASC^{-/-} mice. Two days later, Treg-depleted B6.WT T cells (T_{con}) were transplanted to induce acute GVHD. Although both B6.WT and B6.ASC^{-/-} Tregs attenuated GVHD lethality, their ability to suppress GVHD was identical (Fig. 3B). To examine whether Foxp3^{high}CD4⁺ T cells (CD4⁺ T_{con}) mediated the protection seen in recipients of B6.ASC^{-/-} grafts, we transplanted B6D2F1 recipients with B6.WT TCD BM and CD4⁺ T cells from Treg-depleted B6.WT or B6.ASC^{-/-} donors (Fig. 3C). We observed no difference in survival between these recipients. These data suggest that the survival benefit seen following the transplantation of B6.ASC^{-/-} grafts was unlikely to be a result of effects on CD4⁺ T cells or Tregs in isolation.

ASC controls donor CTL function

Given the exclusion of a primary CD4⁺ T-cell-dependent effect, we speculated that the ASC defect may lie in donor CD8⁺ T cells. We first set-up survival transplants to look at long-term GVHD induction and confirmed that the protection from GVHD seen in recipients of B6.ASC^{-/-} T cells was within the CD8⁺ T-cell compartment (Fig. 3D). Because donor CD8⁺ T-cell numbers were not different after BMT (Fig. 2D), we hypothesized that ASC deficiency may instead alter CTL function. We thus undertook *in vivo* cytotoxicity assays, whereby equivalent numbers of CD45.1⁺ donor-type (B6) and CFSE-labeled host-type (B6D2F1) target cells were cotransferred into CD45.2⁺ B6D2F1 recipients transplanted with B6.WT or B6.ASC^{-/-} (CD45.2⁺) grafts (12 days earlier) to assess the specific clearance of host-type target cells within 18 hours after cell transfer (26). These assays demonstrated an overall reduction of *in vivo* cytotoxicity in recipients of B6.ASC-deficient grafts relative to the recipients of B6.WT grafts (Fig. 3E). Next, we determined that this cytotoxic defect was intrinsic to B6.ASC^{-/-} CD8⁺ T cells by transferring B6.WT CD4⁺ T cells together with either B6.WT or B6.ASC^{-/-} CD8⁺ T cells (Fig. 3F). Further to that, we tested our findings by depleting CD8⁺ T cells from the donor graft and as expected, the increase in cytotoxicity seen in recipients of B6.WT CD8⁺ T cells was eliminated following depletion (Fig. 3G). Given that it has been previously reported that Dock2, a guanine nucleotide-exchange factor required for effective lymphocyte migration and, to a lesser extent, thymocyte development, is deficient in some ASC-knockout lines (7), we sought to confirm

Dock2 and Dock8 expression within naïve B6.WT or B6.ASC^{-/-} CD8⁺ T cells. Our results indicated no difference in expression of either Dock2 or Dock8 irrespective of ASC (Fig. 3H). Together, these data demonstrated that the protection from GVHD seen in the absence of donor ASC was primarily mediated by impairing donor CD8⁺ T cells from acquiring full cytolytic function after BMT.

ASC controls inflammasome-independent gene expression within CTL

To identify the molecular pathways by which ASC controls CTL function after BMT, we performed an RNA microarray, comparing B6.WT and B6.ASC^{-/-} CD8⁺ T cells 12 days posttransplant. Seventeen genes were identified as differentially regulated between B6.WT versus B6.ASC^{-/-} CD8⁺ T cells (represented in a heatmap, Fig. 4A). Next, we performed IPA (303 genes comparing B6.WT vs. B6.ASC^{-/-} CD8⁺ T cells) and identified numerous inflammatory pathways (Supplementary Table S1A), including the GVHD and allograft rejection pathways. Evidence of these immunologic pathways prompted us to analyze the uncorrected dataset, and 10 immunologically relevant genes were differentially regulated in mice transplanted with B6.ASC^{-/-} grafts, including granzyme B (Supplementary Table S1B). To confirm this observation at the protein level, we measured granzyme B secretion in culture supernatants of freshly isolated CD8⁺ T cells posttransplant (Fig. 4B). Indeed, granzyme B protein secretion was reduced in the absence of ASC. Given that granzyme B and perforin act in synergy to induce target cell death, we investigated whether perforin was also altered, but we found expression was not different between B6.WT and B6.ASC^{-/-} CD8⁺ T cells (Fig. 4C). We also measured the cell surface expression of lysosomal marker CD107a to estimate degranulation in the same cells and found it to be diminished when ASC was absent (Fig. 4D). Together, our data suggest that the absence of ASC reduced the capacity of CTLs to induce target cell death by reducing the expression and release of granzyme B.

The microbiome does not impact GVHD outcome in the absence of ASC

It is now known that inflammasome-microbiota interactions play a considerable role in disease outcome (27). Distinctive alteration of the microbiome species between B6.WT and B6.ASC transgenic lines may be attributed to CD8⁺ T-cell function. Changes in the microbiota makeup following irradiation were previously reported to influence GVHD outcome via an inflammasome-dependent mechanism (10). Thus, we cohoused donor B6.WT and B6.ASC^{-/-} mice for 4 weeks, which was sufficient to merge the microbiome between cohoused mice, before utilizing them for BMT (28). Cohousing of mice had no impact on the survival after BMT (Fig. 5A and B). Thus, alterations in the microbiota were not responsible for ASC-mediated GVHD attenuation.

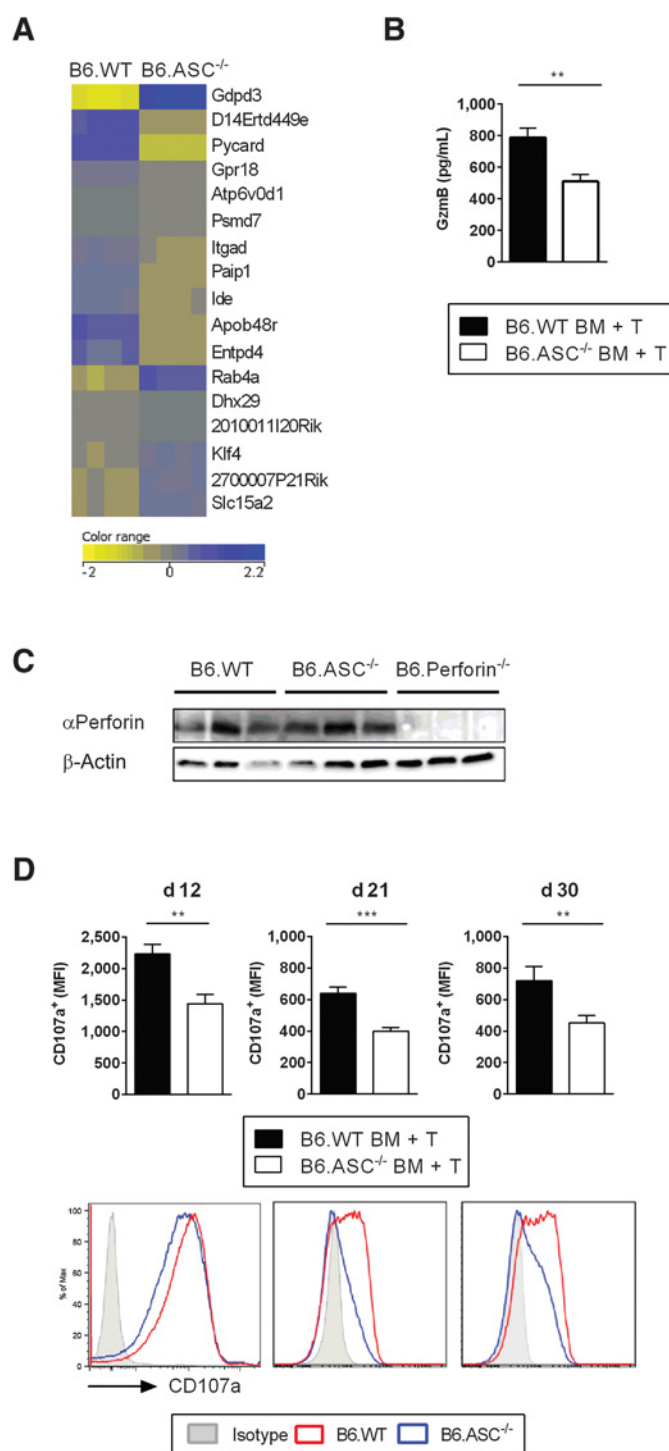
ASC deficiency reduces graft rejection

Given our observations that ASC deficiency impaired donor CD8⁺ T-cell cytotoxic function, we examined its role within the recipient in the context of graft rejection, in which recipient CD8⁺ T cells have a crucial role (29). We utilized a model of graft rejection where we transplanted 1 × 10⁶ luciferase-expressing BALB/c (BALB/c^{luc+}) BM into lethally irradiated B6.WT or B6.ASC^{-/-} recipients. B6.ASC^{-/-} recipients had improved survival (median survival of 47 days vs. 20 days in B6.WT recipients) in conjunction with high levels of engraftment of luciferase-expressing donor cells (Fig. 6A–C). Engraftment, as determined by whole-body luminescence, was similar in ASC- and perforin-deficient recipients (Fig. 6B and C), whereby

ASC Modulates Inflammasome-Independent CTL Cytotoxicity

Figure 4.

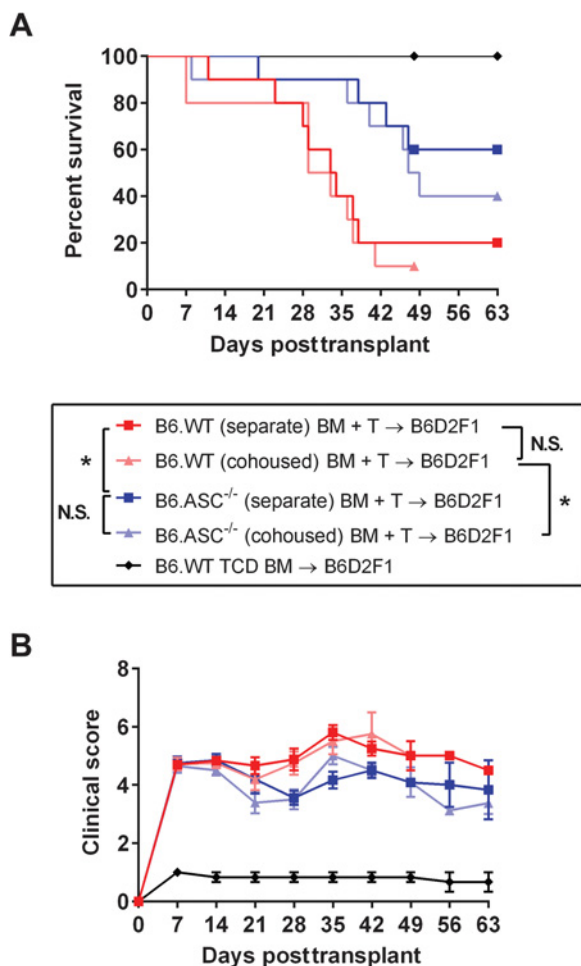
ASC deficiency leads to reduced expression and exocytic release of granzyme B. Lethally irradiated B6D2F1 mice were transplanted with BM and T cells from B6.WT or B6.ASC^{-/-} mice. Splenic CD8⁺ T cells were sorted on day 12 ($n = 4$ per group) and utilized for RNA microarray (**A**) or *ex vivo* cell assays (**B-D**). **A**, After Student *t* test ($P < 0.05$), 304 probes were identified as differentially expressed between B6.WT- versus B6.ASC^{-/-}-sorted CD8⁺ T cells 12 days after transplant (>1.2-fold change cutoff). After Benjamini-Hochberg FDR correction, 17 genes were identified and represented in the heatmap shown. **B**, Splenic CD8⁺ T cells were sorted on day 12 posttransplant and stimulated *ex vivo* (as described in Materials and Methods) for 4 hours before collecting supernatants to measure granzyme B (GzmB) release using an ELISA. Data combined from two experiments ($n = 10$ per group). **C**, Lethally irradiated B6D2F1 mice were transplanted with BM and T cells from B6.WT, B6.ASC^{-/-}, or B6.perforin^{-/-} mice ($n = 3$ per group). Western blot analysis of cell lysates probed for perforin from sorted splenic CD8⁺ T cells. **D**, Whole splenocytes from recipients 12, 21, and 30 days (d) after BMT with B6.WT or B6.ASC^{-/-} BM + T grafts were stimulated *ex vivo* and analyzed for CD107a staining as described in Materials and Methods. Representative CD107a histograms are also shown. Data combined from two experiments for each time point (day 12, $n = 10-12$ per group; day 21, $n = 8-9$ per group; and day 30, $n = 9$ per group). Data were analyzed by Mann-Whitney U test (unpaired, two-tailed). **, $P < 0.01$; ***, $P < 0.001$. Results are presented as mean \pm SEM. MFI, mean fluorescence intensity.



B6.perforin^{-/-} recipients demonstrated superior engraftment rates compared with B6.WT recipients (30), consistent with an advantage for engraftment in the B6.ASC^{-/-} mice. B6.perforin^{-/-} recipients showed complete donor chimerism in all compartments 11 weeks after transplant (**Fig. 6D**). B cells and neutrophils were also almost fully donor derived (>90%) in B6.ASC^{-/-} recipients, whereas mixed donor–host chimerism (50%–60% donor chimerism) was noted within the T-cell compartment (**Fig. 6D**). Surviving B6.WT recipients

rejected the donor grafts, consistent with bioluminescence analysis (**Fig. 6D**). Because recipient NK cells are critical for mediating the early rejection of MHC-mismatched grafts (31, 32), we determined their function in the presence or absence of ASC. We utilized a modified *in vivo* CTL assay that measures NK-cell–dependent cytotoxicity and graft rejection early after transplant (48 hours post-BMT). This assay confirmed NK cells in both B6.WT and B6.ASC^{-/-} recipients to be functionally equivalent (**Fig. 6E**). Given that NK-cell–mediated

Cheong et al.

**Figure 5.**

Microbiota changes after irradiation do not contribute to ASC-mediated GVHD attenuation. **A** and **B**, Lethally irradiated B6D2F1 recipients were transplanted with BM and T cells from donors housed separately or cohoused prior to transplant. A cohort received TCD BM as the non-GVHD control. Survival (**A**) was monitored in conjunction with clinical scoring (**B**) for GVHD manifestations. Results combined from two replicate experiments ($n = 10$ per T-cell-replete group, $n = 6$ for TCD group). *, $P = 0.0243$, B6.ASC^{-/-} versus B6.WT (separate); *, $P = 0.011$, B6.ASC^{-/-} versus B6.WT (cohoused). N.S., not significant. Survival curves were plotted using Kaplan-Meier estimates and compared by log-rank analysis. Results are presented as mean \pm SEM.

rejection occurs within 72 hours of the transplantation of MHC-disparate grafts (32), we postulated that ASC-mediated CD8⁺ T-cell effects are likely to mediate graft rejection at later time points. We thus treated B6.WT and B6.ASC^{-/-} recipients with or without CD8 β -depleting antibody and tracked engraftment by bioluminescence. These studies demonstrated that recipient CD8⁺ T cells, as expected, mediated significant graft rejection and that the defect in graft rejection seen in B6.ASC^{-/-} recipients indeed laid in their CD8⁺ T-cell compartment (Fig. 6F and G).

Graft-versus-leukemia effects can control, but not eradicate, leukemia in the absence of ASC

Because the graft-versus-leukemia (GVL) effect after transplantation is important in determining transplant outcome, we also performed studies investigating leukemia eradication in recipients

of B6.WT or B6.ASC^{-/-} T cells. Lethally irradiated B6D2F1 mice were transplanted with B6.WT TCD BM with or without T cells from B6.WT or B6.ASC^{-/-} mice together with B6D2F1-derived GFP-expressing primary leukemia cells (BCR/ABL-NUP98/HOXA9). We serially analyzed leukemia relapse in peripheral blood by flow cytometry and found that recipients of B6.ASC^{-/-} T cells had a higher leukemia burden 2 to 3 weeks after transplant relative to recipients of B6.WT T cells (Fig. 7A and C). However, B6.ASC^{-/-} T cells eventually controlled leukemia by 4 weeks after BMT (Fig. 7A). As expected, the presence of T cells was required to mediate an effective GVL response because recipients of TCD BM alone developed massive (and lethal) systemic leukemia burden in the blood, BM, and spleen within 14 days of BMT (Fig. 7A and B). Although there was a higher frequency of leukemia present in recipients of donor B6.ASC^{-/-} T cells, we observed progressive reduction in leukemia burden over time (Fig. 7A and C). However, these recipients still exhibited clear evidence of low levels of leukemia in the blood, BM, and spleen 9 weeks post-BMT, although this did not culminate in leukemia-related death (Fig. 7D and E). We also tested the impact of B6.ASC^{-/-} T cells on reactivation of MCMV following BMT. Plasma viremia and viral loads in target organs (Fig. 7F) at day 27 post-transplant (23) were equivalent in mice that received B6.ASC^{-/-} T cells compared with mice that received WT B6 T cells. Taken together, these data demonstrated that B6.ASC^{-/-} donor T cells had a small, but long-term, defect in GVL activity but do not further compromise antiviral immunity.

Discussion

To date, most of the described roles of ASC have focused on caspase-1 inflammasome-dependent innate immunity and autoinflammatory syndromes (33–35). Although the majority of previous studies report a requirement for ASC to control enteric pathogens, others have reported the deleterious effects of ASC in the context of autoimmunity (13, 36, 37). Nonetheless, whether the role of ASC confers protection or induces pathology remains largely dependent on the disease model. An (caspase-1) inflammasome-independent role for ASC has emerged with evidence of cell-extrinsic effects that extend to adaptive immunity. These studies demonstrate various roles for ASC, including increased antigen-induced proliferation of ASC^{+/+} T cells compared with ASC^{-/-} T cells, and its importance for the induction of humoral immunity (38, 39). Other studies have also shown roles for inflammasome-dependent ASC in Th17-mediated pathology (40), and ASC-deficient CD4⁺ T cells have been reported to possess enhanced capacity to suppress bystander T-cell proliferation (41). However, none has reported a role for ASC in mediating CD8⁺ T-cell function and the downstream effects. Our study describes a CD8⁺ T-cell-intrinsic function of ASC in controlling cytolytic function.

A single important study has analyzed the inflammasome in the context of GVHD (10). The authors report that NLRP3^{-/-} and to a much lesser extent ASC^{-/-} recipients showed delayed GVHD onset but commented (in reference to unpublished data) that deficiency in the donor did not appear to influence the severity of GVHD. A small but significant survival advantage was also seen when IL1R^{-/-} T cells were transplanted. Although we did not detect the latter in our systems, IL1 plays an important role in GVHD outcome in animal models (42), such that the inflammasome is likely to be critical and these effects may be mediated through not only donor T cells but also other cell types including dendritic cells (DC; ref. 10). We too demonstrated that NLRP3^{-/-} recipients developed less GVHD but found that an engraftment advantage in the ASC^{-/-} recipients resulted in very similar

ASC Modulates Inflammation-Independent CTL Cytotoxicity

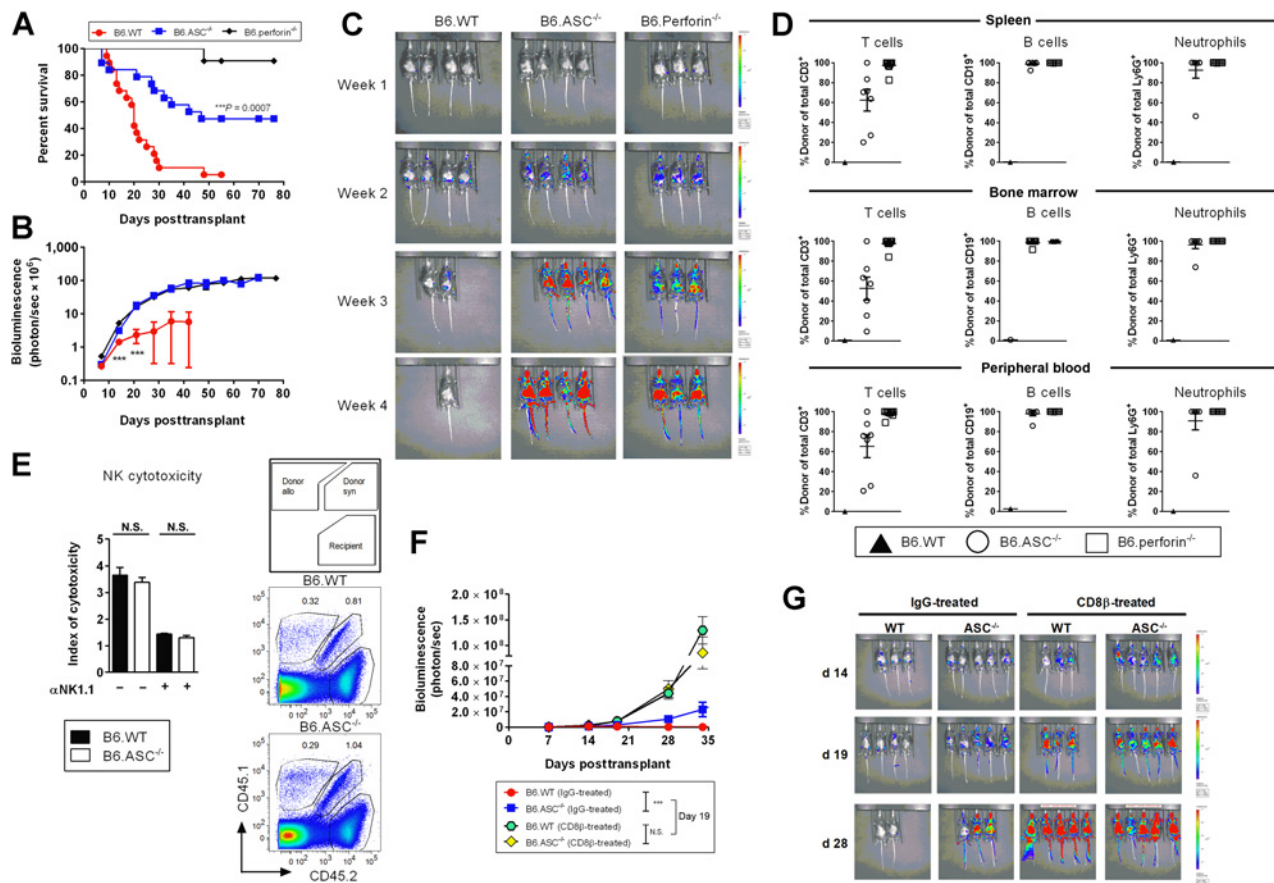


Figure 6.

ASC in recipient $CD8^+$ T cells mediates graft rejection. **A–D**, Lethally irradiated B6.WT, B6.ASC^{-/-}, and B6.perforin^{-/-} recipients were transplanted with luciferase-expressing BALB/c BM. Data are combined from four replicate experiments ($n = 19$ per group for B6.WT and B6.ASC^{-/-}; $n = 11$ per group for B6.perforin^{-/-}). **A**, Survival for the indicated genotypes. *******, $P = 0.0007$, B6.ASC^{-/-} versus B6.WT. Survival curves were plotted using Kaplan–Meier estimates and compared by log-rank analysis. Quantification (**B**) and representative images (**C**) of recipient whole-bioluminescence signals at weeks 1 to 4 after transplant. *******, $P = 0.0003$, B6.ASC^{-/-} versus B6.WT. **D**, Flow cytometric analysis of splenic cells, BM, and peripheral blood at day (d) 80 for donor B-cell, T-cell, and neutrophil engraftment. Data are pooled from three independent experiments (B6.WT, $n = 1$; B6.ASC^{-/-}, $n = 7$; and B6.perforin^{-/-}, $n = 10$). **E**, Lethally irradiated B6.WT and B6.ASC^{-/-} (CD45.2⁺CD45.1⁻) recipients were NK depleted or replete and then transplanted with allogeneic (allo) BM (CD45.1⁺CD45.2⁻) and syngeneic (syn) BM (CD45.1⁺CD45.2⁺). Forty-eight hours later, spleens were analyzed for ratio of CD45.1⁺CD45.2⁻ versus CD45.1⁺CD45.2⁺ populations by flow cytometry. Results combined from three independent experiments ($n = 4–12$ per group). **N.S.**, not significant. **F** and **G**, $CD8^+$ TCD or T-cell-replete recipients were transplanted as in **A**. **F**, Whole-body bioluminescence was quantified thereafter to determine engraftment. Day 19: *******, $P = 0.0003$, B6.ASC^{-/-} versus B6.WT (IgG treated). **N.S.**, not significant. **G**, Representative bioluminescence. Data are representative of two replicate experiments ($n = 10–11$ for B6.WT or B6.ASC^{-/-} groups, $n = 3$ for B6.perforin^{-/-}). All other data were analyzed by Mann–Whitney U test (unpaired, two-tailed). Results are presented as mean \pm SEM.

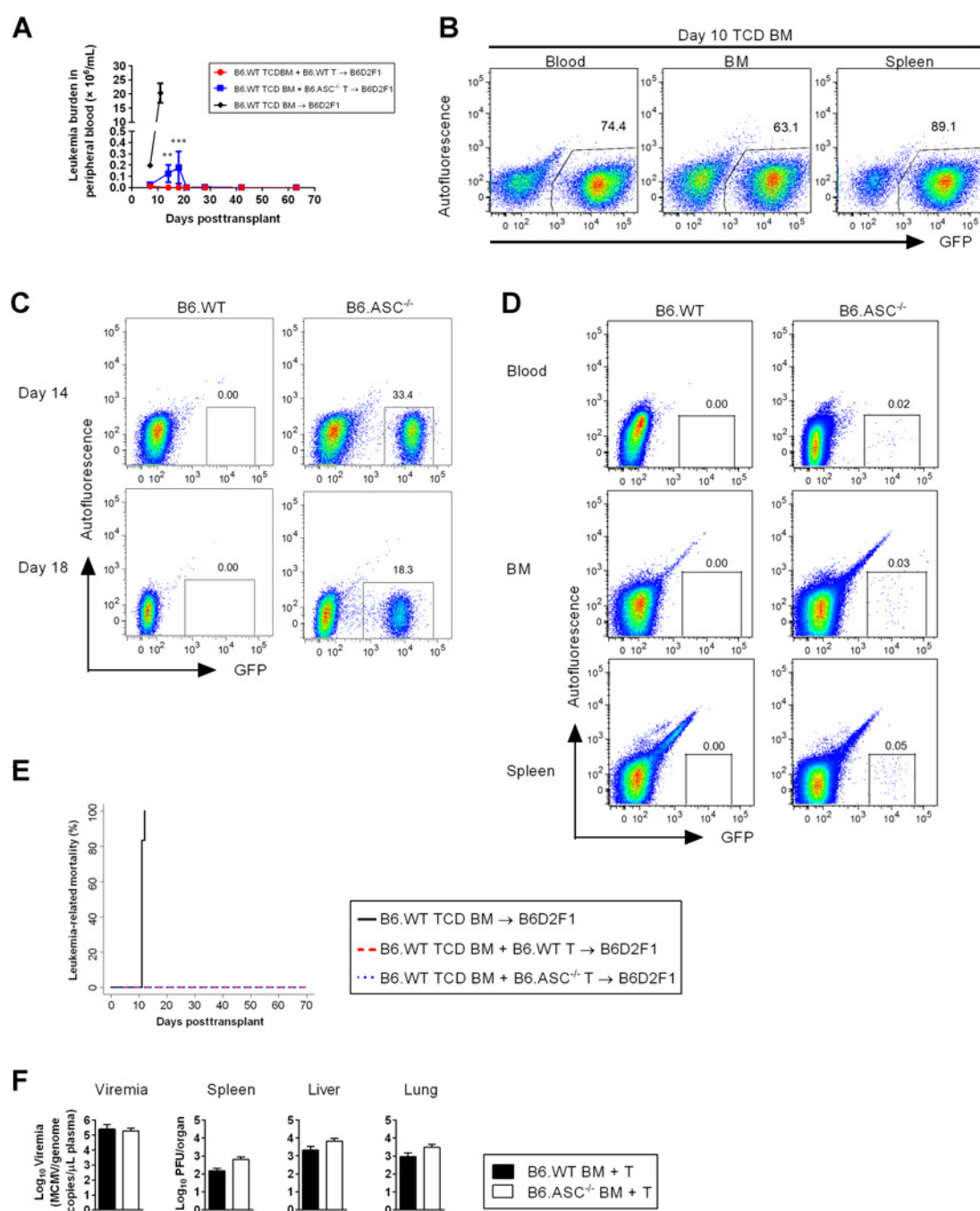
GVHD to WT recipients. We thus used B6D2F1 recipients in our GVHD experiments to minimize effects related to differential engraftment. Perhaps, most importantly, humans have an extensive and diverse microbiome, and the initiators of inflammasome activation (e.g., uric acid) are already well controlled in the clinic. It may, therefore, not be surprising that randomized controlled clinical trials have not demonstrated any benefit for IL1 inhibition in BMT (43). Therefore, the potential pathways involved in inflammasome-independent ASC-mediated GVHD are even more intriguing.

Because it has been shown that abrogating ASC expression influences expression of cytoskeletal proteins, *Dock2* or *Dock8*, within the DC compartment (7, 44), we confirmed neither *Dock2* nor *Dock8* expression in $CD8^+$ T cells was altered in the absence of ASC. Our studies demonstrated an intrinsic defect in cytolytic function, in terms of degranulation within B6.ASC^{-/-} $CD8^+$ T cells that is neither dependent on inflammasome signaling nor microbiota, and suggest

that targeting ASC may offer a greater therapeutic window than inflammasome inhibition *per se*. Because GVHD is the major complication following BMT, inhibition of ASC would perhaps be of greatest benefit early after transplant to minimize GVHD pathology while promoting engraftment, independent of GVL effects. It should be highlighted that the effects seen in this murine model using a genetically deficient ASC^{-/-} mouse will need to be confirmed with selective ASC inhibitors and targeted, conditional ASC deletion with new Cre-flox approaches as these become available.

There are limited studies to date regarding the function of T cells in the presence or absence of ASC. In this study, we showed that the reduced severity of GVHD in the absence of ASC is due to $CD8^+$ T cells and not from $CD4^+$ conventional T cells or Tregs. In spite of a cytolytic defect within ASC-deficient $CD8^+$ T cells, they were still able to maintain significant levels of GVL and antiviral protection, likely via perforin (45). Graft rejection is a major problem in recipients of MHC-

Cheong et al.

**Figure 7.**

GVL effects can control, but not eradicate, leukemia in the absence of ASC. Lethally irradiated B6D2F1 mice were transplanted with B6.WT TCD BM and B6.WT or B6.ASC^{-/-}-sorted CD90.2⁺ T cells and GFP⁺ BCR/ABL-NUP98/HOXA9 leukemia cells. The control group received TCD BM and leukemia cells. **A**, Time course of leukemia burden in peripheral blood ($n = 17$ for T-cell-replete groups, $n = 12$ for TCD group). **, $P = 0.001$; ***, $P = 0.0006$, B6.ASC^{-/-} versus B6.WT. Data combined from three independent experiments. **B**, Representative plots of leukemia (GFP⁺) in the blood, BM, and spleen of TCD BM recipients. **C**, Representative plots of leukemia burden in the blood of recipients at days 14 and 18. **D**, Animals were sacrificed approximately 9 weeks posttransplant and analyzed for leukemia burden in blood, BM, and spleen. Representative plots are shown ($n = 5-6$ per group). **E**, Cumulative incidence of leukemia-related mortality combined from three separate experiments is shown ($n = 17$ per T-cell-replete group, $n = 12$ for TCD group). Data were analyzed by competing risk analysis. **F**, B6D2F1 mice latently infected with MCMV were lethally irradiated and transplanted with BM and T cells from naïve B6.WT or B6.ASC^{-/-} donors. Viremia in the plasma, measured by qRT-PCR, and viral loads in the indicated target organs, determined by plaque assay, at day 27 post-BMT are shown. Data are pooled from two independent experiments ($n = 7-8$ per group). All other data were analyzed by Mann-Whitney U test (unpaired, two-tailed). Results are presented as mean \pm SEM.

ASC Modulates Inflammasome-Independent CTL Cytotoxicity

incompatible grafts in the settings of cord blood and haploidentical transplantation (46, 47), and patients experiencing graft failure have a dismal outcome (48). Although NK cells mediate early graft rejection in this setting, recipient CD8⁺ T cells are an important later effector of disease (29). Our results showed that the absence of recipient ASC expression promotes donor engraftment in a CD8⁺ T-cell-dependent fashion.

In summary, our findings demonstrated a role for ASC in mediating transplant outcome, including GVHD, GVL effects, and graft rejection. Small-molecule inhibitors of NLRP3 within the inflammasome have been generated (49, 50), and this data suggests that similar inhibitors of ASC may serve as particularly attractive therapeutics in both inflammasome- and T-cell-dependent diseases.

Disclosure of Potential Conflicts of Interest

G.R. Hill is a consultant for Generon. No potential conflicts of interest were disclosed by the other authors.

Authors' Contributions

M. Cheong: Conceptualization, formal analysis, funding acquisition, investigation, visualization, methodology, writing—original draft, writing—review and editing. **K.H. Gartlan:** Conceptualization, formal analysis, investigation, visualization, writing—original draft, writing—review and editing. **J.S. Lee:** Conceptualization, formal analysis, investigation, writing—review and editing. **S.-K. Tey:** Investigation, methodology. **P. Zhang:** Formal analysis, investigation. **R.D. Kuns:** Investigation. **C.E. Andoniou:** Conceptualization, investigation, writing—original draft, writing—review and editing. **J.P. Martins:** Formal analysis, investigation, methodology. **K. Chang:** Investigation. **V.R. Sutton:** Formal analysis, investigation, writing—review and editing. **G. Kelly:** Investigation. **A. Varelias:** Formal analysis, investigation. **S. Vuckovic:** Conceptualization,

supervision. **K.A. Markey:** Investigation, methodology, writing—review and editing. **G.M. Boyle:** Formal analysis, writing—review and editing. **M.J. Smyth:** Project administration, writing—review and editing. **C.R. Engwerda:** Conceptualization, resources, supervision, writing—review and editing. **K.P.A. MacDonald:** Conceptualization, investigation. **J.A. Trapani:** Conceptualization, resources, investigation, writing—review and editing. **M.A. Degli-Esposti:** Conceptualization, resources, formal analysis, investigation, visualization, methodology, writing—original draft, writing—review and editing. **M. Koyama:** Conceptualization, formal analysis, supervision, investigation, writing—original draft, writing—review and editing. **G.R. Hill:** Conceptualization, resources, supervision, funding acquisition, writing—original draft, writing—review and editing.

Acknowledgments

This study was supported by research grants from the National Health and Medical Research Council (NHMRC). M. Cheong was a Leukaemia Foundation PhD Fellow. M.J. Smyth was supported by an NHMRC Senior Principal Research Fellowship (1078671) and Investigator Grant (1173958). K.P.A. MacDonald is a Cancer Council of Queensland Fellow. C.R. Engwerda and M.A. Degli-Esposti are NHMRC Principal Research Fellows. J.A. Trapani is a Rosie Lew Fellow of the Peter MacCallum Cancer Foundation. M. Koyama was a Leukaemia Foundation Postdoctoral Fellow. G.R. Hill was an NHMRC Australian Fellow and QLD Health Senior Clinical Research Fellow. The authors thank Paula Hall, Michael Rist, and Grace Chojnowski for cell sorting.

The costs of publication of this article were defrayed in part by the payment of page charges. This article must therefore be hereby marked *advertisement* in accordance with 18 U.S.C. Section 1734 solely to indicate this fact.

Received August 26, 2019; revised February 10, 2020; accepted May 14, 2020; published first May 22, 2020.

References

- Anasetti C, Logan BR, Lee SJ, Waller EK, Weisdorf DJ, Wingard JR, et al. Peripheral-blood stem cells versus bone marrow from unrelated donors. *N Engl J Med* 2012;367:1487–96.
- Blazar BR, Murphy WJ, Abedi M. Advances in graft-versus-host disease biology and therapy. *Nat Rev Immunol* 2012;12:443–58.
- Blazar BR, Hill GR, Murphy WJ. Dissecting the biology of allogeneic HSCT to enhance the GVT effect whilst minimizing GvHD. *Nat Rev Clin Oncol* 2020 Apr 20 [Epub ahead of print].
- Guo H, Callaway JB, Ting JPY. Inflammasomes: mechanism of action, role in disease, and therapeutics. *Nat Med* 2015;21:677–87.
- Broz P, von Moltke J, Jones JW, Vance RE, Monack DM. Differential requirement for caspase-1 autoproteolysis in pathogen-induced cell death and cytokine processing. *Cell Host Microbe* 2010;8:471–83.
- Lin KM, Hu W, Troutman TD, Jennings M, Brewer T, Li X, et al. IRAK-1 bypasses priming and directly links TLRs to rapid NLRP3 inflammasome activation. *Proc Natl Acad Sci U S A* 2014;111:775–80.
- Ippagunta SK, Malireddi RKS, Shaw PJ, Neale GA, Walle LV, Green DR, et al. The inflammasome adaptor ASC regulates the function of adaptive immune cells by controlling Dock2-mediated Rac activation and actin polymerization. *Nat Immunol* 2011;12:1010–6.
- McElvania TeKippe E, Allen IC, Hulseberg PD, Sullivan JT, McCann JR, Sandor M, et al. Granuloma formation and host defense in chronic *Mycobacterium tuberculosis* infection requires PYCARD/ASC but not NLRP3 or caspase-1. *PLoS One* 2010;5:e12320.
- Tsuchiya K, Hara H, Fang R, Hernandez-Cuellar E, Sakai S, Daim S, et al. The adaptor ASC exacerbates lethal *Listeria monocytogenes* infection by mediating IL-18 production in an inflammasome-dependent and -independent manner. *Eur J Immunol* 2014;44:3696–707.
- Jankovic D, Ganesan J, Bscheider M, Stickle N, Weber FC, Guarda G, et al. The Nlrp3 inflammasome regulates acute graft-versus-host disease. *J Exp Med* 2013; 210:1899–910.
- Mariathasan S, Newton K, Monack DM, Vucic D, French DM, Lee WP, et al. Differential activation of the inflammasome by caspase-1 adaptors ASC and Ipaf. *Nature* 2004;430:213–8.
- Glaccum MB, Stocking KL, Charrier K, Smith JL, Willis CR, Maliszewski C, et al. Phenotypic and functional characterization of mice that lack the type I receptor for IL-1. *J Immunol* 1997;159:3364–71.
- Martinson F, Pétrilli V, Mayor A, Tardivel A, Tschopp J. Gout-associated uric acid crystals activate the NALP3 inflammasome. *Nature* 2006;440:237–41.
- Kägi D, Ledermann B, Bürki K, Seiler P, Odermatt B, Olsen KJ, et al. Cytotoxicity mediated by T cells and natural killer cells is greatly impaired in perforin-deficient mice. *Nature* 1994;369:31–7.
- Kuida K, Lippke J, Ku G, Harding M, Livingston D, Su M, et al. Altered cytokine export and apoptosis in mice deficient in interleukin-1 β converting enzyme. *Science* 1995;267:2000–3.
- Cooke K, Kobzik L, Martin T, Brewer J, Delmonte JJ, Crawford J, et al. An experimental model of idiopathic pneumonia syndrome after bone marrow transplantation: I. The roles of minor H antigens and endotoxin. *Blood* 1996;88: 3230–9.
- Dash AB, Williams IR, Kutok JL, Tomasson MH, Anastasiadou E, Lindahl K, et al. A murine model of CML blast crisis induced by cooperation between BCR/ABL and NUP98/HOXA9. *Proc Natl Acad Sci U S A* 2002;99:7622–7.
- Ong ML, Wikstrom ME, Fleming P, Estcourt MJ, Hertzog PJ, Hill GR, et al. CpG pretreatment enhances antiviral T-cell immunity against cytomegalovirus. *Blood* 2013;122:55–60.
- Burman AC, Banovic T, Kuns RD, Clouston AD, Stanley AC, Morris ES, et al. IFN γ differentially controls the development of idiopathic pneumonia syndrome and GVHD of the gastrointestinal tract. *Blood* 2007;110:1064–72.
- MacDonald KP, Rowe V, Filippich C, Thomas R, Clouston AD, Welpy JK, et al. Donor pretreatment with progenipoinetin-1 is superior to granulocyte colony-stimulating factor in preventing graft-versus-host disease after allogeneic stem cell transplantation. *Blood* 2003;101:2033–42.
- Zhang P, Tey SK, Koyama M, Kuns RD, Olver SD, Lineburg KE, et al. Induced regulatory T cells promote tolerance when stabilized by rapamycin and IL-2 in vivo. *J Immunol* 2013;191:5291–303.
- Xu J, Dallas PB, Lyons PA, Shellam GR, Scalzo AA. Identification of the glycoprotein H gene of murine cytomegalovirus. *J Gen Virol* 1992;73:1849–54.

Cheong et al.

23. Martins JP, Andoniou CE, Fleming P, Kuns RD, Schuster IS, Voigt V, et al. Strain-specific antibody therapy prevents cytomegalovirus reactivation after transplantation. *Science* 2019;363:288–93.
24. Schuster IS, Wikstrom ME, Brizard G, Coudert JD, Estcourt MJ, Manzur M, et al. TRAIL+ NK cells control CD4+ T cell responses during chronic viral infection to limit autoimmunity. *Immunity* 2014;41:646–56.
25. Kayagaki N, Warming S, Lamkanfi M, Vande Walle L, Louie S, Dong J, et al. Non-canonical inflammasome activation targets caspase-11. *Nature* 2011;479:117–21.
26. Morris ES, MacDonald KP, Rowe V, Banovic T, Kuns RD, Don AL, et al. NKT cell-dependent leukemia eradication following stem cell mobilization with potent G-CSF analogs. *J Clin Invest* 2005;115:3093–103.
27. Ayres JS. Inflammasome-microbiota interplay in host physiologies. *Cell Host Microbe* 2013;14:491–7.
28. Varelias A, Ormerod KL, Bunting MD, Koyama M, Gartlan KH, Kuns RD, et al. Acute graft-versus-host disease is regulated by an IL-17-sensitive microbiome. *Blood* 2017;129:2172–85.
29. Koyama M, Hashimoto D, Nagafuji K, Eto T, Ohno Y, Aoyama K, et al. Expansion of donor-reactive host T cells in primary graft failure after allogeneic hematopoietic SCT following reduced-intensity conditioning. *Bone Marrow Transplant* 2014;49:110–5.
30. Taylor MA, Ward B, Schatzle JD, Bennett M. Perforin- and Fas-dependent mechanisms of natural killer cell-mediated rejection of incompatible bone marrow cell grafts. *Eur J Immunol* 2002;32:793–9.
31. Westerhuis G, Maas WG, Willemze R, Toes RE, Fibbe WE. Long-term mixed chimerism after immunologic conditioning and MHC-mismatched stem-cell transplantation is dependent on NK-cell tolerance. *Blood* 2005;106:2215–20.
32. Hamby K, Trexler A, Pearson TC, Larsen CP, Rigby MR, Kean LS. NK cells rapidly reject allogeneic bone marrow in the spleen through a perforin- and Ly49D-dependent, but NKG2D-independent mechanism. *Am J Transplant* 2007;7:1884–96.
33. Dey N, Sinha M, Gupta S, Gonzalez MN, Fang R, Endsley JJ, et al. Caspase-1/ASC inflammasome-mediated activation of IL-1 β -ROS-NF- κ B pathway for control of *Trypanosoma cruzi* replication and survival is dispensable in NLRP3-/- macrophages. *PLoS One* 2014;9:e111539.
34. Gov L, Karimzadeh A, Ueno N, Lodoen MB. Human innate immunity to *Toxoplasma gondii* is mediated by host caspase-1 and ASC and parasite GRA15. *MBio* 2013;4:e00255–13.
35. Broderick L, De Nardo D, Franklin BS, Hoffman HM, Latz E. The inflammasome and autoinflammatory syndromes. *Annu Rev Pathol* 2015;10:395–424.
36. Shaw PJ, Lukens JR, Burns S, Chi H, McGargill MA, Kanneganti TD. Cutting edge: critical role for PYCARD/ASC in the development of experimental autoimmune encephalomyelitis. *J Immunol* 2010;184:4610–4.
37. Wen H, Gris D, Lei Y, Jha S, Zhang L, Huang MT, et al. Fatty acid-induced NLRP3-ASC inflammasome activation interferes with insulin signaling. *Nat Immunol* 2011;12:408–15.
38. Kolly L, Karababa M, Joosten LA, Narayan S, Salvi R, Pétrilli V, et al. Inflammatory role of ASC in antigen-induced arthritis is independent of caspase-1, NALP-3, and IPAF. *J Immunol* 2009;183:4003–12.
39. Ellebedy AH, Lupfer C, Ghoneim HE, DeBeauchamp J, Kanneganti TD, Webby RJ. Inflammasome-independent role of the apoptosis-associated speck-like protein containing CARD (ASC) in the adjuvant effect of MF59. *Proc Natl Acad Sci U S A* 2011;108:2927–32.
40. Martin BN, Wang C, Zhang CJ, Kang Z, Gulen MF, Zepp JA, et al. T cell-intrinsic ASC critically promotes TH17-mediated experimental autoimmune encephalomyelitis. *Nat Immunol* 2016;17:583–92.
41. Narayan S, Kolly L, So A, Busso N. Increased interleukin-10 production by ASC-deficient CD4+ T cells impairs bystander T-cell proliferation. *Immunology* 2011;134:33–40.
42. Hill GR, Teshima T, Gerbitz A, Pan L, Cooke KR, Brinson YS, et al. Differential roles of IL-1 and TNF-alpha on graft-versus-host disease and graft versus leukemia. *J Clin Invest* 1999;104:459–67.
43. Antin JH, Weisdorf D, Neuberger D, Nicklow R, Clouthier S, Lee SJ, et al. Interleukin-1 blockade does not prevent acute graft-versus-host disease: results of a randomized, double-blind, placebo-controlled trial of interleukin-1 receptor antagonist in allogeneic bone marrow transplantation. *Blood* 2002;100:3479–82.
44. Krishnaswamy JK, Singh A, Gowthaman U, Wu R, Gorrepati P, Sales Nascimento M, et al. Coincidental loss of DOCK8 function in NLRP10-deficient and C3H/HeJ mice results in defective dendritic cell migration. *Proc Natl Acad Sci U S A* 2015;112:3056–61.
45. Tsukada N, Kobata T, Aizawa Y, Yagita H, Okumura K. Graft-versus-leukemia effect and graft-versus-host disease can be differentiated by cytotoxic mechanisms in a murine model of allogeneic bone marrow transplantation. *Blood* 1999; 93:2738–47.
46. Tang BL, Zhu XY, Zheng CC, Liu HL, Geng LQ, Wang XB, et al. Successful early unmanipulated haploidentical transplantation with reduced-intensity conditioning for primary graft failure after cord blood transplantation in hematologic malignancy patients. *Bone Marrow Transplant* 2015;50:248–52.
47. Ruggeri A, Labopin M, Sormani MP, Sanz G, Sanz J, Volt F, et al. Engraftment kinetics and graft failure after single umbilical cord blood transplantation using a myeloablative conditioning regimen. *Haematologica* 2014;99:1509–15.
48. Olsson RF, Logan BR, Chaudhury S, Zhu X, Akpek G, Bolwell BJ, et al. Primary graft failure after myeloablative allogeneic hematopoietic cell transplantation for hematologic malignancies. *Leukemia* 2015;29:1754–62.
49. Primiano MJ, Lefker BA. Efficacy and pharmacology of the NLRP3 inflammasome inhibitor CP-456,773 (CRID3) in murine models of dermal and pulmonary inflammation. *J Immunol* 2016;197:2421–33.
50. Jiang H, He H, Chen Y, Huang W, Cheng J, Ye J, et al. Identification of a selective and direct NLRP3 inhibitor to treat inflammatory disorders. *J Exp Med* 2017;214: 3219–38.

Cancer Immunology Research

ASC Modulates CTL Cytotoxicity and Transplant Outcome Independent of the Inflammasome

Melody Cheong, Kate H. Gartlan, Jason S. Lee, et al.

Cancer Immunol Res 2020;8:1085-1098. Published OnlineFirst May 22, 2020.

Updated version Access the most recent version of this article at:
doi:[10.1158/2326-6066.CIR-19-0653](https://doi.org/10.1158/2326-6066.CIR-19-0653)

Supplementary Material Access the most recent supplemental material at:
<http://cancerimmunolres.aacrjournals.org/content/suppl/2020/05/22/2326-6066.CIR-19-0653.DC1>

Cited articles This article cites 49 articles, 23 of which you can access for free at:
<http://cancerimmunolres.aacrjournals.org/content/8/8/1085.full#ref-list-1>

E-mail alerts [Sign up to receive free email-alerts](#) related to this article or journal.

Reprints and Subscriptions To order reprints of this article or to subscribe to the journal, contact the AACR Publications Department at pubs@aacr.org.

Permissions To request permission to re-use all or part of this article, use this link
<http://cancerimmunolres.aacrjournals.org/content/8/8/1085>.
Click on "Request Permissions" which will take you to the Copyright Clearance Center's (CCC) Rightslink site.